Interfacial Stresses in RC Beams Strengthened by Externally Bonded FRP/Steel Plates with Effects of Shear Deformations

Mahmoud Edalati[1] and Fereidoon Irani[2]

Abstract: This paper introduces an analytical method to calculate the interfacial shear and normal stresses in reinforced concrete (RC) beams strengthened by a fiber reinforced polymer (FRP) sheet or a steel plate (i.e., a soffit plate). The maximum interfacial shear and normal stresses are localized at the end of the soffit plate, and as a result, a debonding phenomenon develops at this position and may produce a sudden failure of the structure. The effects of the shear deformations are calculated in an RC beam, an adhesive layer, and a soffit plate. Thus, the composite RC beam is assumed to be a Timoshenko beam. Application of shear deformations to a Timoshenko beam results in a pair of simultaneous second-order and fourth-order ordinary differential equations. In the engineering literature, these equations are called coupled differential equations. These coupled equations are solved analytically considering all terms. The present paper illustrates the effects of interfacial stresses on the behavior of RC structures strengthened by FRP sheets or steel plates. Finally, the agreement of the results obtained from the analytical solution and the results available in the literature confirms the accuracy of the proposed approach in predicting both interfacial shear and normal stresses. **DOI: 10.1061/(ASCE)CC.1943-5614.0000238.** © *2012 American Society of Civil Engineers.*

CE Database subject headings: Concrete beams; Reinforced concrete; Fiber reinforced polymer; Steel; Plates; Shear stress; Shear deformation; Analytical techniques.

Author keywords: Concrete beams; Reinforced concrete; Fiber reinforced polymer; Steel; Plates; Shear stress; Shear deformation; Analytical techniques.

Introduction

Reinforced concrete (RC) beams can be strengthened with a soffit plate (a fiber reinforced polymer [FRP] sheet or a steel plate). The adherence of these sheets to the concrete beams is one of several general methods for strengthening RC beams (Smith and Teng 2001). The strength of the bonding between the soffit plate and the concrete is an important parameter that in part determines the behavior of RC beams. Many researchers have published experimental results and analytical analyses showing that the distributions of the interfacial shear and normal stresses on both sides of the sticky surfaces and the debonding phenomena between the soffit plate and the concrete interface are extremely complex (Smith and Teng 2001; Yang and Wu 2007). However, in the last two decades, those same researchers have published several analytical solutions, but they have not reported analytical solutions regarding how the shear deformation influences the interfacial stresses (Smith and Teng 2001).

In structures retrofitted with FRP sheets or steel plates, the debonding of the plate ends is considered a challenging failure mode because it prevents the beam from reaching its full bending moment capacity. Therefore, determining the debonding failure load is important. The debonding phenomenon depends on the magnitude and the concentration of shear and normal stresses between the soffit plate and the RC beam interface (Smith and Teng 2001). This is the reason why significant research on RC beams strengthened with FRP sheets or steel plates has focused on this matter for the last two decades. Some closed-form methods exist that use simple relations for the interfacial shear and normal stresses (Smith and Teng 2001; Yang and Wu 2007; Tounsi et al. 2009; Roberts 1989; Roberts and Haji-Kazemi 1989; Malek et al. 1998). These relations are based on simplifying assumptions related to the adhesive layer. The writers focus here on the assumption that the interfacial shear and normal stresses are constant on both sides of the adhesive layer.

Numerous analytical and numerical studies of this system have been carried out; some studies have incorporated both analytical and numerical methods. Some of the most important works in this field are Vilnay (1988), Roberts (1989), Roberts and Haji-Kazemi (1989), Oehlers and Moran (1990), Saadatmanesh and Ehsani (1991), Oehlers (1992), Chajes et al. (1994), Taljsten (1997), Saadatmanesh and Malek (1998), Malek et al. (1998), Etman and Beeby (2000), Rabinovitch and Frostig (2000, 2001), Chen and Teng (2001), Maalej and Bian (2001), Ye (2001), Shen et al. (2001), Smith and Teng (2001), Teng et al. (2002), Yang et al. (2004), Maalej and Leong (2005), Wu et al. (2005), Tounsi (2006), Yuan et al. (2007), Yang and Wu (2007), Li et al. (2009), Tounsi et al. (2009), and Zhang and Teng (2010). Smith and Teng (2001) completed a practical comparative study on the assumptions, advantages, and disadvantages of the most important methods used for determining the interfacial shear and normal stresses. Most of these investigations failed to consider the axial, bending, and shear deformations simultaneously. In addition, in some of the studies,

[1]Assistant Professor in Structural Engineering, Dept. of Civil Engineering, Ilam Univ., Ilam, Iran; formerly, Ph.D. Candidate in Structural Engineering, Dept. of Civil Engineering, Ferdowsi Univ. of Mashhad, Mashhad, Iran (corresponding author). E-mail: edalati.mahmoud@mail.ilam.ac.ir and edalati.mahmoud@yahoo.com

[2]Professor of Structural Engineering, Dept. of Civil Engineering, Ferdowsi Univ. of Mashhad, Mashhad, Iran. E-mail: irani@um.ac.ir

Note. This manuscript was submitted on January 24, 2011; approved on June 14, 2011; published online on June 16, 2011. Discussion period open until July 1, 2012; separate discussions must be submitted for individual papers. This paper is part of the ***Journal of Composites for Construction***, Vol. 16, No. 1, February 1, 2012. ©ASCE, ISSN 1090-0268/2012/1-60–73/$25.00.

the effect of the shear deformation is not specifically considered in the beam, in the adhesive layer, or in the soffit plate. In some papers, the coupled differential equations have been changed into uncoupled ones, and the resulting solutions are insufficiently accurate. Although Smith and Teng (2001) and Yang and Wu (2007) have introduced and solved the governing differential equations, the former paper neglected the effect of the shear deformation to obtain uncoupled equations, and the latter divided the differential equations into two parts (with and without the shear deformation effect) and used Fourier series to expand the shear deformation. Superposition and the Galerkin method were used to obtain the solutions to the differential equations (Yang and Wu 2007).

Several high-order analytical solutions exist to determine the interfacial shear and normal stresses (Rabinovitch and Frostig 2000; Shen et al. 2001). It should be also noted that the solution of Rabinovitch and Frostig (2000) does not provide explicit expressions for the interfacial stresses. In this solution the constants of integration are not given and only the boundary conditions are listed. Then it seems impossible to obtain any result to develop a design rule (Smith and Teng 2001; Shen et al. 2001). The correctness of this analysis has also been questioned (Shen et al. 2001; Smith and Teng 2001). In another high-order analysis that is introduced by Shen et al. (2001), some other explicit expressions have been obtained but the relations do not consider the effects of shear deformation and shear curvature in the composite beam. It is well known that Timoshenko's theory is a refined beam theory that takes shear deformation into account (Antes 2003).

In this paper, the shear deformations in the beam, the adhesive layer and the soffit plate were included to determine the interfacial shear and the normal stresses. Because the Timoshenko beam theory was used, some terms were added to the differential equations presented by other researchers. This paper introduces an analytical solution for determining the interfacial shear and the normal stresses without eliminating any term in the coupled differential equations. The Timoshenko beam assumption makes it possible to use this solution for both ordinary beams and short-span beams (while considering the shear deformations). To reduce the shear rigidity, especially in short-span beams, the equivalent flexural rigidity should be used instead of the actual flexural rigidity. Disregarding this reduction coefficient leads to incorrect results in short-span beams with a span-to-depth ratio less than five and to an inaccurate solution in ordinary beams. In beams with a sandwichlike construction, the increase in the deflection attributable to the shear deformation effect may be as great as 50% (Gere and Timoshenko 1984). An increase in the deformation before debonding causes a significant rise in the interfacial shear and the normal stresses, particularly between sandwich layers. In a strengthened Timoshenko RC beam, the shear curvature should be added to the bending curvature.

Differences between the key points of this work with other researchers' papers are:

- In the method of Smith and Teng (2001) the factor of curve slope for vertical normal stress in Eq. (20) has been removed to achieve a simple solution and noninvolving differential equations.
- All factors that have shear shape coefficient have been eliminated in differential equations of Smith and Teng (2001) [see the explicit responses of the interfacial shear and vertical normal stresses in Smith and Teng (2001)].
- In the present paper the Shear curvatures of RC beam and soffit plate (composite beam curvature) and effects of the shear shape factor on the flexural and shear rigidities in involved differential equations [i.e., Eqs. (44)], are taken into account. None of these effects are taken into consideration in Smith and Teng's paper (2001) or papers of other researchers.
- The main difference of this paper with the other researchers' work and even with high-order methods [Shen et al. (2001) and Rabinovitch and Frostig (2000)] lies in applying of Bernoulli beam theory in findings of all other researchers and using the Timoshenko composite beam theory in this paper.

Assumptions

A simple RC beam of length L is subjected to an arbitrary distributed load of density $q(x)$ along its unit length, as shown in Fig. 1(a). The beam is strengthened along a portion of its midspan with the help of an adhesive layer and an FRP sheet or a steel plate of length L_p. The distance of the beam supports from the soffit plate is equal to L_{fs}. No limitations exist on the type of strengthening materials that can be used; another suitable plate may replace the soffit plate. The dimensions of the beam cross-section are shown in Fig. 1(b), in which b_1 and b_2 are the widths of the RC beam and the soffit plate, respectively ($b_2 \leq b_1$) In this study, the width b_a of the adhesive layer is equal to the width b_2 of the soffit plate. In addition, in Fig. 1(b), d_1, d_2, and t_a are the thicknesses of the RC beam, the soffit plate, and the adhesive layer, respectively. Note that in Fig. 1, the subscripts 1 and 2 are used for the RC beam and the soffit plate, respectively.

The following assumptions were used to obtain the governing expressions [Smith and Teng (2001), Roberts (1989), and Roberts and Haji-Kazemi (1989)]:

- All materials exhibit linear elastic behavior, and the effect of steel reinforcement in concrete has been neglected (Tounsi et al. 2009);

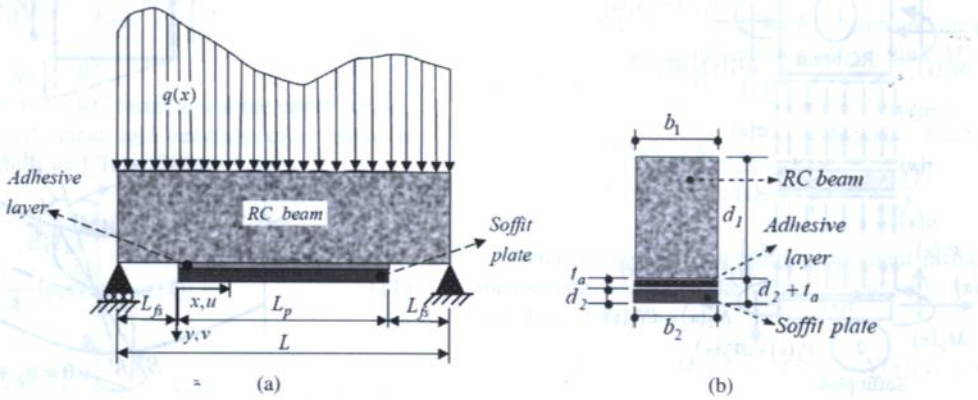

Fig. 1. (a) Simple RC beam strengthened by a soffit plate under a distributed load; (b) cross-section of a composite beam

- Deformations attributable to bending moments and axial and shear forces are considered in the behavior of both the RC beam and the soffit plate;
- The effect of normal stresses on the thickness of the adhesive layer is neglected and, consequently, the curvatures of the RC beam and the soffit plate are assumed to be the same;
- The continuity exists between the soffit plate and the RC beam; and
- The effects of bending deformations are neglected in the adhesive layer.

This paper does not satisfy the zero shear stress condition at the end of adhesive layer, which is known to have only a negligible effect in a very small zone near the end of the plate (Smith and Teng 2001; Roberts 1989). The obtained results by Shen et al. (2001), Teng et al. (2002), Yang et al. (2009), and Zhang and Teng (2010) prove once again that the above condition has only a minor effect at the 2 mm end of the soffit plate.

It is important to declare that in this paper the interfacial stress is under consideration only at the middle of adhesive thickness [i.e., the midadhesive (MA) interface] so it does not determine the interfacial stress either in the adhesive-to-concrete (AC) interface or in the plate-to-adhesive (PA) interface.

Governing Equations for Interfacial Shear Stress between an RC Beam and a Soffit Plate

Fig. 2 shows the beam, the adhesive layer, and the soffit plate separately. In this figure, the axial and shear forces, together with the bending moments, are represented by $N_j(x)$, $V_j(x)$, and $M_j(x)$, respectively. The interfacial shear and normal stresses are represented by $\tau(x)$ and $\sigma(x)$, respectively. Subscripts $j = 1$ and $j = 2$ define the RC beam and the soffit plate, respectively. The shear strain γ in the adhesive layer may be represented by (Smith and Teng 2001):

$$\gamma = \frac{du(x,y)}{dy} + \frac{dv(x,y)}{dx} \tag{1}$$

in which $u(x,y)$ and $v(x,y)$ = horizontal and vertical displacements, respectively, at any point from the adhesive layer. The origin for the x-axis and y-axis is located at the end of the soffit plate, as shown in Fig. 1.

The interfacial shear stress $\tau(x)$, which is related to the shear strain γ, may be derived from Eq. (1):

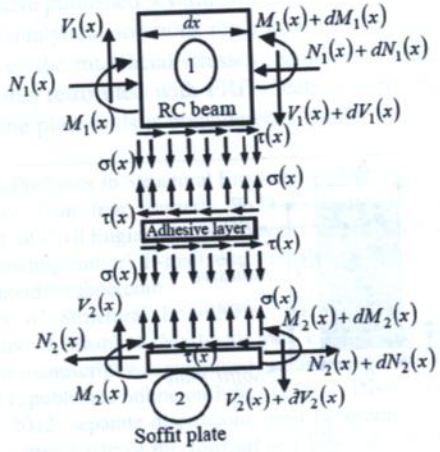

Fig. 2. Differential segments in a cross-section of a composite beam

$$\tau(x) = G_a\gamma = G_a\left[\frac{du(x,y)}{dy} + \frac{dv(x,y)}{dx}\right] \tag{2}$$

in which G_a = shear modulus of the adhesive layer. The first derivative of Eq. (2) with respect to x is as follows:

$$\frac{d\tau(x)}{dx} = G_a\left[\frac{d^2u(x,y)}{dxdy} + \frac{d^2v(x,y)}{dx^2}\right] \tag{3}$$

The curvature of a differential segment under the shear deformation effect may be defined using Fig. 3. The effect of shear curvature has not been investigated in flexural strengthen RC beams by externally bonded FRP/steel plates. Thus, the type of influence discussed in this paper is a new research matter.

The bending curvature $(\frac{d\theta_b}{dx})$, the shear curvature $(\frac{d\theta_s}{dx})$, and the total curvature $(\frac{d\theta}{dx})$ may be written as follows:

$$\begin{cases} \dfrac{d\theta_b}{dx} = \dfrac{d^2v_b(x,y)}{dx^2} = \dfrac{-M_T(x)}{(EI)_t} \\ \dfrac{d\theta_s}{dx} = \dfrac{d^2v_s(x,y)}{dx^2} = \dfrac{-1}{(\alpha GA)_t}\dfrac{dV_T(x)}{dx} \\ \dfrac{d\theta}{dx} = \dfrac{d^2v(x,y)}{dx^2} = \dfrac{d\theta_b}{dx} + \dfrac{d\theta_s}{dx} \end{cases} \tag{4}$$

in which $v_b(x,y)$, $v_s(x,y)$, and $v(x,y)$ = bending, shear, and total deformations in a cross-section of the beam; $V_T(x)$ and $M_T(x)$ = total shear force and the total bending moment in the composite section, respectively; $(\alpha GA)_t$ and $(EI)_t$ - effective shear rigidity and the effective flexural rigidity in the total composite section, which may be obtained from the following relationships (Gere and Timoshenko 1984; Stafford and Coull 1991):

$$\begin{cases} (\alpha GA)_t = \alpha(G_1A_1 + G_2A_2) \\ (EI)_t = E_1I_1 + E_2I_2 \\ I_1 = \dfrac{I_{1b}}{1 + r_{1e}} \\ I_2 = \dfrac{I_{2b}}{1 + r_{2e}} \end{cases} \tag{5}$$

in which E_j, I_j, G_j, and A_j = modulus of elasticity, the reduced effective moment of inertia with respect to the centroid, the shear modulus, and the cross-sectional area in the jth segment, respectively; α = shape factor for the shear [for solid rectangular cross-section: $\alpha = 10(1+\nu)/(12+11\nu)$; ν = Poisson's ratio;

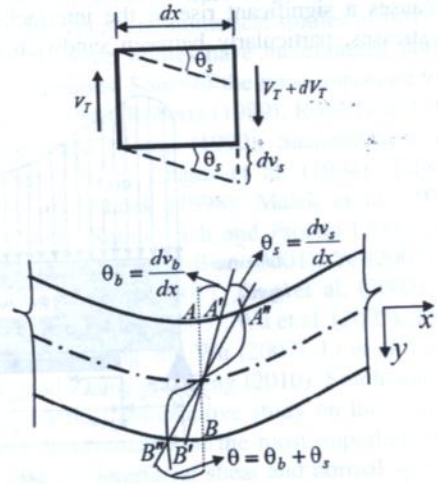

Fig. 3. Bending and shear curvatures in a Timoshenko composite beam

Cowper 1966] and its value is approximately equal to $\frac{5}{6}$ in rectangular sections (Gere and Timoshenko 1984); I_{1b} and I_{2b} = moments of inertia in the RC beam and the soffit plate (Stafford and Coull 1991). In Eq. (5), r_{1e} and r_{2e} are determined, respectively, through bending deflection curve and the additional deflection of shear deformation in RC beam and soffit plate. These quantities are the factor of reduction for second moment of cross-sectional area. It is clear that the maximal influence of these two are at $x = \frac{L_p}{2}$. In this paper r_{1e} and r_{2e} are used at $x = \frac{L_p}{2}$ to simplify the solution of differential equations. Consequently, by simplifying the deflection curve these two factors are determined by the following equations (Gere and Timoshenko 1984):

$$\begin{cases} \beta_1 = \dfrac{L_{fs}+x}{L} \\ \gamma_1 = \dfrac{192E_1I_{1b}}{5\alpha G_1A_1L^2} \\ r_{1e} = \dfrac{16}{5}(\beta_1^4 - 2\beta_1^3 + \beta_1) + \gamma_1(\beta_1 - \beta_1^2) - 1 \left(r_{1e} = \dfrac{48E_1I_{1b}}{5\alpha G_1A_1L^2} \text{ at } x = \dfrac{L_p}{2} \right) \\ \beta_2 = \dfrac{L_{fs}+x}{L_p} \\ \gamma_2 = \dfrac{192E_2I_{2b}}{5\alpha G_2A_2L_p^2} \\ r_{2e} = \dfrac{16}{5}(\beta_2^4 - 2\beta_2^3 + \beta_2) + \gamma_2(\beta_2 - \beta_2^2) - 1 \left(r_{2e} = \dfrac{48E_2I_{2b}}{5\alpha G_2A_2L_p^2} \text{ at } x = \dfrac{L_p}{2} \right) \end{cases} \tag{6}$$

Thus, the total curvature of a differential segment in a strengthened Timoshenko RC beam can be expressed as follows:

$$\frac{d^2v(x,y)}{dx^2} = \frac{d\theta_b}{dx} + \frac{d\theta_s}{dx} = -\frac{M_T(x)}{(EI)_t} - \frac{1}{(\alpha GA)_t}\frac{dV_T(x)}{dx} \tag{7}$$

Assuming that the adhesive layer is subjected to uniform interfacial shear stresses, the variations of $u(x,y)$ in the thickness of the adhesive layer will be linear, yielding (Smith and Teng 2001):

$$\frac{du(x,y)}{dy} = \frac{1}{t_a}[u_2(x) - u_1(x)] \tag{8}$$

The second derivative of Eq. (8) with respect to x is

$$\frac{d^2u(x,y)}{dxdy} = \frac{1}{t_a}\left[\frac{du_2(x)}{dx} - \frac{du_1(x)}{dx}\right] \tag{9}$$

in which $u_1(x)$ and $u_2(x)$ = longitudinal deformations at the bottom of RC beam and the upper surface of soffit plate, respectively. The thickness of the adhesive layer is t_a. Using Eqs. (7) and (9) in Eq. (3), yields

$$\frac{d\tau(x)}{dx} = \frac{G_a}{t_a}\left[\frac{du_2(x)}{dx} - \frac{du_1(x)}{dx} - \frac{t_a}{(EI)_t}M_T(x) - \frac{t_a}{(\alpha GA)_t}\frac{dV_T(x)}{dx}\right] \tag{10}$$

The strain at the bottom of the RC beam and at the upper surface of the soffit plate under axial, shear, and bending deformations is determined as follows (Smith and Teng 2001):

$$\frac{du_1(x)}{dx} = \varepsilon_1(x) = \frac{y_1}{E_1I_1}M_1(x) - \frac{1}{E_1A_1}N_1(x) + \frac{y_1}{\alpha G_1A_1}[q(x) + b_2\sigma(x)] \tag{11}$$

$$\frac{du_2(x)}{dx} = \varepsilon_2(x) = -\frac{y_2}{E_2I_2}M_2(x) + \frac{1}{E_2A_2}N_2(x) + \frac{y_2}{\alpha G_2A_2}b_2\sigma(x) \tag{12}$$

in which $\varepsilon_1(x)$ and $\varepsilon_2(x)$ = axial strain at the bottom surface of the RC beam and at the upper surface of the soffit plate, respectively; $N_j(x)$ and $M_j(x)$ = axial force and the bending moment in the jth segment, applied at distance $y_j (j = 1, 2)$; y_1 and y_2 = distances of the RC beam centroid from its bottom and of the centroid of the soffit plate from its upper surface. The relationship between y_1 and y_2 given d_1 and d_2 is as follows:

$$y_1 = \frac{d_1}{2} \tag{13}$$

$$y_2 = \frac{d_2}{2} \tag{14}$$

The horizontal equilibrium of the composite segment gives

$$\frac{dN_1(x)}{dx} = \frac{dN_2(x)}{dx} = b_2\tau(x) \tag{15}$$

in which

$$N_1(x) = N_2(x) = N(x) = b_2\int_0^x \tau(x)dx \tag{16}$$

Because the curvature of the RC beam and the adhesive layer are equal, the relationship between $M_1(x)$ and $M_2(x)$ is as follows (Smith and Teng 2001):

$$\frac{M_1(x)}{E_1I_1} = \frac{M_2(x)}{E_2I_2} \Rightarrow \begin{cases} M_1(x) = RM_2(x) \\ R = \dfrac{E_1I_1}{E_2I_2} \end{cases} \tag{17}$$

Determining the total bending moment in the differential segments with respect to the center of the soffit plate yields (Smith and Teng 2001):

$$M_T(x) = M_1(x) + M_2(x) + N(x)(y_1 + y_2 + t_a) \tag{18}$$

in which the bending moments at the RC beam and the soffit plate are (Smith and Teng 2001)

$$M_1(x) = \frac{R}{R+1}\left[M_T(x) - b_2\int_0^x \tau(x)(y_1+y_2+t_a)dx\right] \quad (19)$$

$$M_2(x) = \frac{1}{R+1}\left[M_T(x) - b_2\int_0^x \tau(x)(y_1+y_2+t_a)dx\right] \quad (20)$$

The first derivative of Eqs. (19) and (20) with respect to x gives

$$\frac{dM_1(x)}{dx} = V_1(x) = \frac{R}{R+1}[V_T(x) - b_2\tau(x)(y_1+y_2+t_a)] \quad (21)$$

$$\frac{dM_2(x)}{dx} = V_2(x) = \frac{1}{R+1}[V_T(x) - b_2\tau(x)(y_1+y_2+t_a)] \quad (22)$$

Substituting Eqs. (11) and (12) into Eq. (10) gives:

$$\frac{d\tau(x)}{dx} = \frac{G_a}{t_a}\left\{-\frac{y_2}{E_2I_2}M_2(x) + \frac{1}{E_2A_2}N_2(x) + \frac{y_2}{\alpha G_2A_2}b_2\sigma(x) - \frac{y_1}{E_1I_1}M_1(x) + \frac{1}{E_1A_1}N_1(x) - \frac{y_1}{\alpha G_1A_1}[q + b_2\sigma(x)] - \frac{t_a}{(EI)_t}M_T(x) - \frac{t_a}{(\alpha GA)_t}\frac{dV_T(x)}{dx}\right\} \quad (23)$$

Differentiating the above expression with respect to x and substituting Eqs. (15)–(22) into Eq. (23) yields

$$\frac{d^2\tau(x)}{dx^2} - a_0\tau(x) + b_0\frac{d\sigma(x)}{dx} = f(x) \quad (24)$$

in which the constants a_0 and b_0 and function $f(x)$ are defined as follows:

$$a_0 = \frac{G_ab_2}{t_a}\left[\frac{(y_1+y_2)(y_1+y_2+t_a)}{E_1I_1+E_2I_2} + \frac{1}{E_1A_1} + \frac{1}{E_2A_2}\right] \quad (25)$$

$$b_0 = \frac{G_ab_2}{\alpha t_a}\left(\frac{y_1}{G_1A_1} - \frac{y_2}{G_2A_2}\right) \quad (26)$$

$$f(x) = -\frac{G_a}{t_a}\left[\frac{y_1+y_2}{E_1I_1+E_2I_2} + \frac{t_a}{(EI)_t}\right]V_T(x) - \frac{G_a}{t_a}\frac{y_1}{\alpha G_1A_1}\frac{dq}{dx} - \frac{G_a}{(\alpha GA)_t}\frac{d^2V_T(x)}{dx^2} \quad (27)$$

Note that the terms with the subscript t in Eq. (27) have not been considered by other researchers. Eq. (24) is the governing differential equation for interfacial shear stress between an RC beam and a soffit plate.

Governing Equations for Interfacial Normal Stress between an RC Beam and a Soffit Plate

Creation of vertical separation between the RC beam and the soffit plate under the applied loading leads to the governing differential equation for interfacial normal stress. The vertical separation may initiate normal stresses $[\sigma(x)]$ in the adhesive layer, which may be obtained by following equation (Smith and Teng 2001):

$$\sigma(x) = \frac{E_a}{t_a}[v_2(x) - v_1(x)] \quad (28)$$

in which E_a = elastic modulus of the adhesive layer; and $v_1(x)$ and $v_2(x)$ = vertical deformation at the bottom of the RC beam or at the upper surface of the soffit plate. Writing the equilibrium equations for the RC beam and the soffit plate and neglecting the second-order and higher order terms obtains the following expressions (Smith and Teng 2001).

For the RC beam:

$$\frac{d^2v_1(x)}{dx^2} = -\frac{1}{E_1I_1}M_1(x) - \frac{1}{\alpha G_1A_1}[q(x) + b_2\sigma(x)] \quad (29)$$

$$\frac{dM_1(x)}{dx} = V_1(x) - b_2y_1\tau(x) \quad (30)$$

$$\frac{dV_1(x)}{dx} = -b_2\sigma(x) - q(x) \quad (31)$$

For the soffit plate:

$$\frac{d^2v_2(x)}{dx^2} = -\frac{1}{E_2I_2}M_2(x) + \frac{1}{\alpha G_2A_2}b_2\sigma(x) \quad (32)$$

$$\frac{dM_2(x)}{dx} = V_2(x) - b_2y_2\tau(x) \quad (33)$$

$$\frac{dV_2(x)}{dx} = b_2\sigma(x) \quad (34)$$

Consecutively differentiating Eqs. (29) and (32) and using Eqs. (30), (31), (33), and (34), the following expressions are obtained.

For the RC beam:

$$\frac{d^4v_1(x)}{dx^4} = \frac{1}{E_1I_1}b_2\sigma(x) + \frac{1}{E_1I_1}q(x) + \frac{b_2y_1}{E_1I_1}\frac{d\tau(x)}{dx} - \frac{1}{\alpha G_1A_1}\frac{d^2q(x)}{dx^2} - \frac{b_2}{\alpha G_1A_1}\frac{d^2\sigma(x)}{dx^2} \quad (35)$$

For the soffit plate:

$$\frac{d^4v_2(x)}{dx^4} = -\frac{1}{E_2I_2}b_2\sigma(x) + \frac{b_2y_2}{E_2I_2}\frac{d\tau(x)}{dx} + \frac{b_2}{\alpha G_2A_2}\frac{d^2\sigma(x)}{dx^2} \quad (36)$$

Substituting Eqs. (35) and (36) into the forth-order derivative of Eq. (28) will be:

$$\frac{d^4\sigma(x)}{dx^4} - c_0\frac{d^2\sigma(x)}{dx^2} + d_0\sigma(x) + e_0\frac{d\tau(x)}{dx} = g(x) \quad (37)$$

in which constants c_0, d_0, and e_0 and function $g(x)$ are defined as follows:

$$c_0 = \frac{E_a}{t_a}\frac{b_2}{\alpha}\left(\frac{1}{G_1A_1} + \frac{1}{G_2A_2}\right) \quad (38)$$

$$d_0 = \frac{E_a}{t_a}b_2\left(\frac{1}{E_1I_1} + \frac{1}{E_2I_2}\right) \quad (39)$$

$$e_0 = \frac{E_a}{t_a}b_2\left(\frac{y_1}{E_1I_1} - \frac{y_2}{E_2I_2}\right) \quad (40)$$

$$g(x) = \frac{E_a}{t_a}\left[\frac{1}{\alpha G_1A_1}\frac{d^2q(x)}{dx^2} - \frac{1}{E_1I_1}q(x)\right] \quad (41)$$

Eq. (37) is the governing differential equation for the interfacial normal stress between an RC beam and a soffit plate.

General Solutions for the Coupled Differential Governing Equations for Interfacial Stresses

By using the differential governing equations for interfacial shear and normal stresses simultaneously [i.e., Eqs. (24) and (37)] the resulting coupled differential governing equations are as follows:

$$\begin{cases} \dfrac{d^2\tau(x)}{dx^2} - a_0\tau(x) + b_0\dfrac{d\sigma(x)}{dx} = f(x) \\ \dfrac{d^4\sigma(x)}{dx^4} - c_0\dfrac{d^2\sigma(x)}{dx^2} + d_0\sigma(x) + e_0\dfrac{d\tau(x)}{dx} = g(x) \end{cases} \tag{42}$$

in which a_0, b_0, c_0, d_0, and e_0 and functions $f(x)$ and $g(x)$ are already defined. The coupled differential equations in Eq. (42) are ordinary inhomogeneous differential equations. Defining the parameters

$$D = \frac{d}{dx}, \quad D^2 = \frac{d^2}{dx^2}, \quad D^4 = \frac{d^4}{dx^4}, \quad \tau = \tau(x), \quad \sigma = \sigma(x) \tag{43}$$

Eq. (42) can be rewritten

$$D^2\tau - a_0\tau + b_0 D\sigma = f(x) \tag{44a}$$

$$D^4\sigma - c_0 D^2\sigma + d_0\sigma + e_0 D\tau = g(x) \tag{44b}$$

On multiplying $-e_0 D$ by Eq. (44*a*), $(D^2 - a_0)$ by Eq. (44*b*), it is possible to eliminate the interfacial shear stress τ in the inhomogeneous coupled differential equations [Eq. (44)]. Thus

$$[D^6 - (a_0 + c_0)D^4 + (a_0c_0 + d_0 - b_0e_0)D^2 - a_0d_0]\sigma = \underbrace{(D^2 - a_0)g(x) - e_0Df(x)}_{F(x)} \tag{45}$$

The characteristic equation related to the above expression is as follows:

$$\lambda^6 - (a_0 + c_0)\lambda^4 + (a_0c_0 + d_0 - b_0e_0)\lambda^2 - a_0d_0 = 0 \tag{46}$$

Using a change of variables, $m = \lambda^2$, obtains

$$m^3 - (a_0 + c_0)m^2 + (a_0c_0 + d_0 - b_0e_0)m - a_0d_0 = 0 \tag{47}$$

Solving the characteristic equation [Eq. (47)] gives the following eigenvalues:

$$\begin{cases} m_1 = \dfrac{1}{3}\left[a_0 + c_0 - \dfrac{\sqrt[3]{2}n_2}{n_1} + \dfrac{n_3}{\sqrt[3]{2}}\right] \\ m_2 = \dfrac{1}{3}\left[a_0 + c_0 + \dfrac{(1 + i\sqrt{3})n_2}{\sqrt[3]{4}n_3} - \dfrac{(1 - i\sqrt{3})n_3}{2\sqrt[3]{2}}\right] \\ m_3 = \dfrac{1}{3}\left[a_0 + c_0 + \dfrac{(1 - i\sqrt{3})n_2}{\sqrt[3]{4}n_3} - \dfrac{(1 + i\sqrt{3})n_3}{2\sqrt[3]{2}}\right] \end{cases} \tag{48}$$

in which $i = \sqrt{-1}$; and n_1, n_2 and n_3 are defined below:

$$\begin{cases} n_1 = 2a_0^3 - 3a_0^2c_0 - 3a_0c_0^2 + 2c_0^3 + 18a_0d_0 - 9c_0d_0 + 9a_0b_0e_0 + 9b_0c_0e_0 \\ n_2 = -a_0^2 + a_0c_0 - c_0^2 + 3d_0 - 3b_0e_0 \\ n_3 = \sqrt[3]{n_1 + \sqrt{n_1^2 + 4n_2^3}} \end{cases} \tag{49}$$

Therefore, the interfacial normal stress $\sigma(x)$ is expressed as Eq. (50):

$$\sigma(x) = C_1e^{-\sqrt{m_1}x} + C_2e^{\sqrt{m_1}x} + C_3e^{-\sqrt{m_2}x} + C_4e^{\sqrt{m_2}x} + C_5e^{-\sqrt{m_3}x} + C_6e^{\sqrt{m_3}x} - \frac{F(x)}{a_0d_0} \tag{50}$$

in which $F(x)$ = function of the applied load on the beam and is determined by the following equation [see Eq. (45)]:

$$F(x) = (D^2 - a_0)g(x) - e_0Df(x) \tag{51}$$

Multiplying the Eq. (44*a*) by $(D^4 - c_0D^2 + d_0)$, Eq. (44*b*) by $-b_0D$ results to eliminate σ in the coupled differential equations [Eq. (44)]. Then

$$[D^6 - (a_0 + c_0)D^4 + (a_0c_0 + d_0 - b_0e_0)D^2 - a_0d_0]\tau = \underbrace{(D^4 - c_0D^2 + d_0)f(x) - b_0Dg(x)}_{G(x)} \tag{52}$$

The characteristic equation for Eq. (52) is the same as Eq. (46). Therefore, the relation for the interfacial shear stress $\tau(x)$ is obtained using Eq. (53):

$$\tau(x) = K_1e^{-\sqrt{m_1}x} + K_2e^{\sqrt{m_1}x} + K_3e^{-\sqrt{m_2}x} + K_4e^{\sqrt{m_2}x} + K_5e^{-\sqrt{m_3}x} + K_6e^{\sqrt{m_3}x} - \frac{G(x)}{a_0} \tag{53}$$

in which $G(x)$ depends on the loading condition on the beam. Therefore [see Eq. (52)]

$$G(x) = (D^4 - c_0D^2 + d_0)f(x) - b_0Dg(x) \tag{54}$$

By simultaneous substitution of Eqs. (50) and (53) into one of the coupled differential equations [Eq. (44)], the constants K_1 through K_6 can be calculated as functions of C_1 through C_6:

$$\begin{cases} K_{2j-1} = \dfrac{b_0C_{2j-1}\sqrt{m_j}}{m_j - a_0} \\ K_{2j} = -\dfrac{b_0C_{2j}\sqrt{m_j}}{m_j - a_0} \end{cases} \quad j = 1, 2, 3 \tag{55}$$

Finally, the relationship of $\tau(x)$ to C_1 through C_6 is as follows:

$$\tau(x) = \frac{b_0 C_1 \sqrt{m_1}}{m_1 - a_0} e^{-\sqrt{m_1}x} - \frac{b_0 C_2 \sqrt{m_1}}{m_1 - a_0} e^{\sqrt{m_1}x} + \frac{b_0 C_3 \sqrt{m_2}}{m_2 - a_0} e^{-\sqrt{m_2}x} - \frac{b_0 C_4 \sqrt{m_2}}{m_2 - a_0} e^{\sqrt{m_2}x} + \frac{b_0 C_5 \sqrt{m_3}}{m_3 - a_0} e^{-\sqrt{m_3}x} - \frac{b_0 C_6 \sqrt{m_3}}{m_3 - a_0} e^{\sqrt{m_3}x} - \frac{G(x)}{a_0} \tag{56}$$

Eqs. (50) and (56) are the general solutions of the coupled differential governing equations [i.e., Eqs. (42) or (44)] for this problem.

Boundary Conditions

Calculating the General Boundary Conditions

Although all the relationships obtained in this paper for the stresses in the RC beam and the soffit plate interface are in general form, the authors chose to explore the case of a uniformly distributed load (UDL) in full detail. It was decided to determine the analytical solutions related to two other types of loading (e.g., one and two concentrated loads). The boundary conditions, which are related to the interfacial shear and the normal stresses in each case, may be established depending on the type of external loading.

The relations of the total shear force and the total bending moment, in the case of UDL [$q(x) = q =$ constant.] are as follows:

$$\begin{cases} V_T(x) = \frac{q}{2}(L_P - 2x) \\ M_T(x) = \frac{q}{2}[x(L_P - x) + L_{fs}(L_P + L_{fs})] \end{cases} \quad 0 \le x \le L_P \tag{57}$$

Substitution of the boundary conditions $N_1(0) = N_2(0) = M_2(0) = 0$; $\frac{dV_T(0)}{dx} = -q$; $M_1(0) = M_T(0) = \frac{qL_{fs}}{2}(L_P + L_{fs})$ into Eq. (23) gives Eq. (58*a*). Once again, substitution of Eq. (29), Eq. (32), $M_1(0)$, and $M_T(0)$ into the second derivative of Eq. (28) with respect to x gives Eq. (58*b*). Finally substitution of the third derivative of Eqs. (29) and (32) with respect to x into the right side of the third derivative of Eq. (28) with respect to x and using the boundary conditions $V_1(0) = \frac{qL_P}{2}$; $V_2(0) = 0$ and $\frac{d^3q(x)}{dx^3} = 0$ arrives at Eq. (58*c*). Thus the boundary conditions will be as follows:

$$b_0\sigma(x)|_{x=0} + \left.\frac{d\tau(x)}{dx}\right|_{x=0} = ff + gg \tag{58a}$$

$$-c_0\sigma(x)|_{x=0} + \left.\frac{d^2\sigma(x)}{dx^2}\right|_{x=0} = hh + mm \tag{58b}$$

$$e_0\tau(x)|_{x=0} - c_0\left.\frac{d\sigma(x)}{dx}\right|_{x=0} + \left.\frac{d^3\sigma(x)}{dx^3}\right|_{x=0} = nn + rr \tag{58c}$$

in which ff, gg, hh, mm, nn, and rr are given as follows:

$$\begin{cases} ff = -\frac{G_a}{t_a}\left(\frac{y_1}{E_1 I_1} + \frac{t_a}{(EI)_t}\right) M_T(x)|_{x=0}, \\ hh = \frac{E_a}{t_a}\left(\frac{1}{E_1 I_1}\right) M_T(x)|_{x=0}, \\ nn = \frac{E_a}{t_a}\left(\frac{1}{E_1 I_1}\right) V_T(x)|_{x=0}, \end{cases} \quad \begin{aligned} gg &= -\frac{G_a}{\alpha t_a}\left(\frac{y_1}{G_1 A_1} - \frac{t_a}{(GA)_t}\right) q(x)|_{x=0} \\ mm &= \frac{E_a}{\alpha t_a}\left(\frac{1}{G_1 A_1}\right) q(x)|_{x=0} \\ rr &= \frac{E_a}{\alpha t_a}\left(\frac{1}{G_1 A_1}\right) \left.\frac{dq(x)}{dx}\right|_{x=0} \end{aligned} \tag{59}$$

The three boundary conditions in Eq. (58) are general and are independent of the loadings at the ends of the soffit plate.

Determination of the Particular Boundary Conditions

When a UDL is applied to the full span of an RC beam, the shear stress in the midspan of the beam (i.e., the midspan of the soffit plate) is zero:

$$\tau(x)\big|_{x=\frac{L_P}{2}} = 0 \tag{60}$$

Calculating Constants C_1 through C_6 in the UDL Case

For large values of x, the normal stress is supposed to approach zero. The numerical coefficients related to the two constants C_4 and C_6 that can be obtained by Eq. (58) at $x = L_p$ are very large. Therefore, the two constants C_4 and C_6 become zero. This is similar to the two constants C_3 and C_4 in Eq. (36) of reference Smith and Teng (2001). C_4 and C_6 being zero, Eq. (60) may be used instead of Eq. (58) at the other end of soffit plate (i.e., $x = L_p$). The other constants (i.e., C_1, C_2, C_3, and C_5) can be determined with the help of Eqs. (58) and (60). C_2 is equal to zero and C_1, C_3, and C_5 are expressed in terms of the other constants E_1, E_2, E_a, G_1, G_2, G_a, b_1, b_2, d_1, d_2, t_a, q, L, and L_p. A hypothetical function H_j was chosen as follows:

$$C_j = H_j(E_1, E_2, E_a, G_1, G_2, G_a, b_1, b_2, d_1, d_2, t_a, q, L, L_p); \quad j = 1, 3, 5 \tag{61}$$

The analytical relationships for C_1, C_3, and C_5 can be found in the appendix.

Numerical Examples and Verifications

The following numerical examples show the efficiency of the presented method using a computer program written by the writers. In this section, two examples are discussed. The first is a simple RC beam strengthened by a GFRP/CFRP sheet or a steel plate. This beam is subjected to a uniformly distributed load (UDL) $q(x) = q = 50$ N/mm over its full span. The beam span is $L = 3,000$ mm, and the distance of the soffit plate from the supports is $L_{fs} = 300$ mm. The second example is an aluminum (Al) box beam with a wall thickness equal to 2 mm that is strengthened by a CFRP sheet. This beam is subjected to a UDL equal to $q(x) = q = 2$ N/mm. The span length and the distance of the soffit plate from the supports are $L = 500$ mm and $L_{fs} = 50$ mm, respectively. The other geometric and material properties of the beams, the soffit plates (i.e., GFRP/CFRP sheet or steel plate), and the adhesive layer are listed in Table 1. Roberts (1989), Roberts and Haji-Kazemi (1989), Malek et al. (1998), Smith and Teng (2001),

Table 1. Geometric and Material Properties for the Beams, the Adhesive Layer, and the Soffit Plates

Components	Width (mm)	Depth (mm)	Elasticity modulus (MPa)	Poisson's ratio	Shear modulus
RC beam	$b_1 = 200$	$d_1 = 300$	$E_1 = 30{,}000$	$\upsilon_1 = 0.20$	$G_1 = 12{,}500$
Al beam	$b_1 = 20$	$d_1 = 30$	$E_1 = 65{,}300$	$\upsilon_1 = 0.33$	$G_1 \approx 24{,}550$
Adhesive layer (RC beam)	$b_a = 200$	$t_a = 2$	$E_a = 2000$	$\upsilon_a = 0.35$	$G_a \approx 740$
Adhesive layer (Al beam)	$b_a = 20$	$t_a = 2$	$E_a = 2{,}000$	$\upsilon_a = 0.35$	$G_a \approx 740$
GFRP sheet (RC beam)	$b_2 = 200$	$t_2 = 4$	$E_2 = 50{,}000$	$\upsilon_2 = 0.30$	$G_2 \approx 19{,}230$
CFRP sheet (RC beam)	$b_2 = 200$	$t_2 = 4$	$E_2 = 100{,}000$	$\upsilon_2 = 0.30$	$G_2 \approx 38{,}460$
Steel plate (RC beam)	$b_2 = 200$	$t_2 = 4$	$E_2 = 200{,}000$	$\upsilon_2 = 0.30$	$G_2 = 76{,}920$
CFRP sheet (Al beam)	$b_2 = 20$	$t_2 = 4$	$E_2 = 100{,}000$	$\upsilon_2 = 0.30$	$G_2 = 38{,}460$

and Yong and Wu (2007) have already analyzed these examples using various analytical solutions.

Example One: RC Beam with a GFRP/CFRP/Steel Soffit Plate under a UDL

In this example, the RC beam is strengthened by a GFRP/CFRP sheet or a steel plate and carries a UDL. In Figs. 4–6, the interfacial shear and normal stresses are plotted at the beginning of the soffit plate (in the short range $0 \le x \le 0.025L_p$) for a GFRP sheet, a CFRP sheet, and a steel plate, respectively. The results obtained from the analytical solution in this paper are in good agreement with the Smith and Teng (2001) solution. The main difference between these solutions occurs at the ends of the soffit plate and is attributable to the shear deformation effect. The shear effect is exerted in the present analytical solution but is not considered by Smith and Teng (2001) or in other analytical solutions. It was noted that, at the end of the soffit plate, the sign of the interfacial normal stress changes. The change in the sign of the normal stress is attributable to the extra bending deformations of the soffit plates by interfacial shear stresses. The shear deformation has much more influence on the shear stresses than on the normal stresses. Therefore, the shear deformation has a pronounced effect on the increase of the shear stresses. It therefore plays a significant role in the debonding phenomenon and in load failure.

Although the results of both methods are similar, the results obtained from the present method are more accurate because they take into account the shear deformation effects in the coupled differential governing equations. Table 2 indicates the numerical values of the maximum interfacial shear stress (τ_{max}) and normal stress (σ_{max}) obtained by different methods. These stresses occur at the ends of the soffit plate. In addition to the shear deformation effect, if the effect of the reduced second moment of area in this

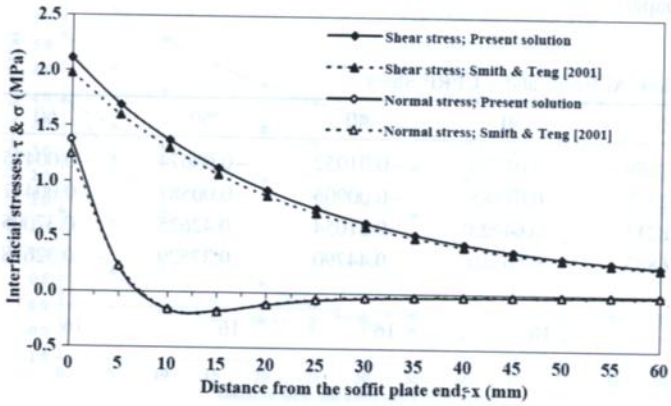

Fig. 4. Distribution of the interfacial shear and normal stresses between an RC beam and a GFRP sheet

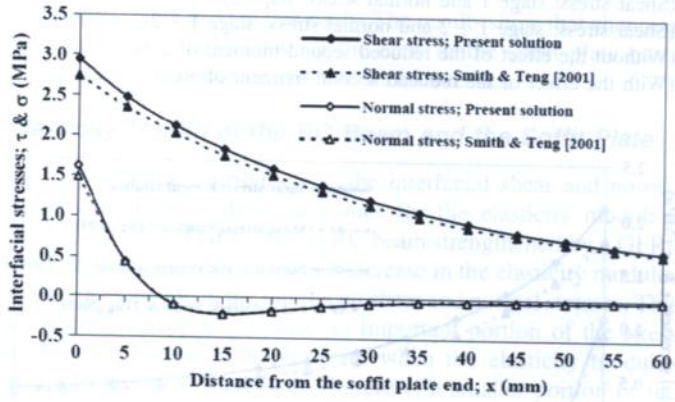

Fig. 5. Distribution of the interfacial shear and normal stresses between an RC beam and a CFRP sheet

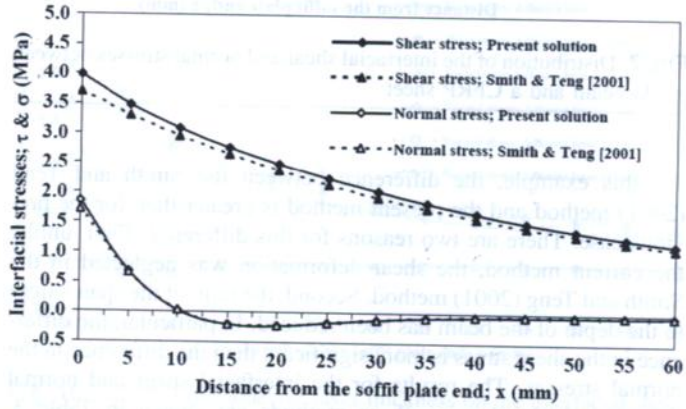

Fig. 6. Distribution of the interfacial shear and normal stresses between an RC beam and a steel plate

deformation is considered the difference between the previous solutions and the present solution is considerable (see the last row of Table 2). In particular, the effect of the shear stress and its influence on the bending rigidity in soffit plates with high rigidity is not negligible (for instance, the steel plate). Therefore, the results regarding the interfacial stress, and especially the shear stress, are significant.

Example 2: Hollow Al Beam with a CFRP Soffit Plate under a UDL

Fig. 7 shows the distribution of interfacial shear and normal stresses at the end of a CFRP sheet bonded to a simply supported hollow aluminum beam with a wall thickness of 2 mm. This beam is subjected to a UDL. It was analyzed using the analytical methods recommended by Smith and Teng (2001) and the current procedure.

Table 2. Comparison of the Maximum Interfacial Shear and Normal Stresses in Examples 1 and 2 (in MPa)

Analytical method	RC beam with GFRP sheet		RC beam with CFRP sheet		RC beam with steel plate		Al beam with CFRP sheet	
	τ_{max}	σ_{max}	τ_{max}	σ_{max}	τ_{max}	σ_{max}	τ_{max}	σ_{max}
Roberts and Haji-Kazemi[a](1989)	2.001	1.425	2.776	1.668	3.745	1.902	2.079	1.153
Roberts and Haji-Kazemi[b] (1989)	1.813	1.256	2.591	1.500	3.567	1.733	1.962	1.060
Roberts (1989)	1.945	1.386	2.604	1.567	3.302	1.683	1.552	0.910
Malek et al. (1998)	1.943	1.384	2.597	1.563	3.287	1.675	1.499	0.871
Smith and Teng (2001)	1.975	1.244	2.740	1.484	3.696	1.713	1.796	0.930
Yang and Wu (2007)	1.955	1.227	2.684	1.472	3.592	1.695	1.748	0.917
Present[c]	2.112	1.376	2.946	1.621	3.982	1.853	2.103	1.082
Present[d]	2.168	1.413	3.021	1.662	4.078	1.898	2.131	1.097

[a](Shear stress: stage 1 and normal stress: stage 2).
[b](Shear stress: stage 1 + 2 and normal stress: stage 1 + 2).
[c](Without the effect of the reduced second moment of area).
[d](With the effect of the reduced second moment of area).

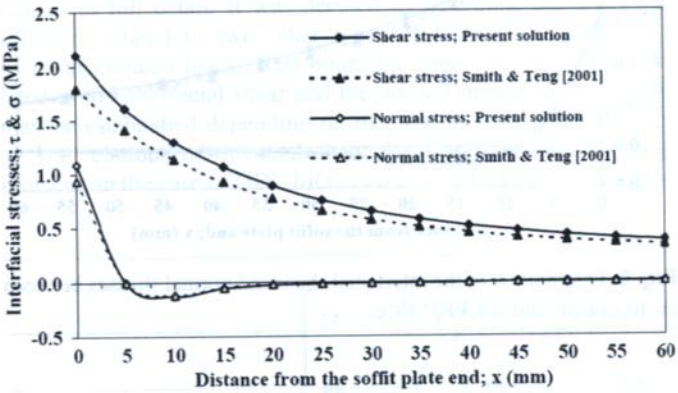

Fig. 7. Distribution of the interfacial shear and normal stresses between an Al beam and a CFRP sheet

For this example, the difference between the Smith and Teng (2001) method and the present method is greater than for the previous case. There are two reasons for this difference. First, unlike the current method, the shear deformation was neglected in the Smith and Teng (2001) method. Second, the ratio of the span length to the depth of the beam has been reduced. In particular, the difference in the shear stress is more significant than the difference in the normal stresses. The results for the interfacial shear and normal stresses calculated using these methods are shown in Table 3. The percentage difference between the results obtained from these methods is also shown in Table 3. The results show that the absolute values of the maximum and minimum differences in the shear stresses for the studied length are 17 and 13%, respectively, and these percentages for the normal stresses are 22 and 7%. Significant differences exist between both methods, particularly for the maximum shear stress.

The values of the maximum interfacial shear and normal stresses in the aluminum beam are presented in the last two columns of Table 2. This value is 1.42 times higher than the lowest value, which was obtained by Malek et al. (1998). Moreover, the highest and lowest values of the interfacial normal stresses can be found in the solutions of Roberts and Haji-Kazemi (1989) and Malek et al. (1998), respectively. Their ratio is 1.32 in this case. The differences between the results of this example obtained from the present solution and from the solution of Roberts and Haji-Kazemi (1989) (stages: 1 + 2) are approximately 2.5 and 5% for the interfacial normal and shear stresses, respectively.

It is obvious that for a simple beam with a shear deformations effect (a Timoshenko beam), the displacements increase with respect to the ordinary (Euler-Bernoulli) beam. Therefore, the tendency for the soffit plates and the principle beam to slide is higher. As the values of the second moment of area and the shear cross-sectional area decrease because of the shear deformation effect, the interfacial stresses may increase in each case. This increase is confirmed by the finite element method (Li et al. 2009; Zhang and Teng 2010). Yang and Wu (2007) and Tounsi et al. (2009) illustrate that selecting hypothetical functions for modeling the behavior of an interfacial material results in smaller values for the shear and normal stresses in comparison with the results obtained from other papers.

Table 3. Comparison of the Interfacial Shear and Normal Stress between a Hollow Al Beam and a CFRP Sheet

x (mm)	0.0	10	20	30	40	50	60
$\sigma_{Present}$ (MPa)	1.08207	−0.13013	−0.02889	−0.01720	−0.01052	−0.00674	−0.00475
$\sigma_{Smith\ and\ Teng\ (2001)}$ (MPa)	0.92953	−0.12179	−0.02372	−0.01485	−0.00906	−0.00581	−0.00411
$\tau_{Present}$ (MPa)	2.10289	1.29277	0.88213	0.64723	0.51054	0.42625	0.37005
$\tau_{Smith\ and\ Teng\ (2001)}\beta$ (MPa)	1.79556	1.13184	0.76883	0.56580	0.44790	0.37529	0.32678
$\left\lvert\frac{\sigma_{Present}-\sigma_{Smith\ and\ Teng\ (2001)}}{\sigma_{Smith\ and\ Teng\ (2001)}}\right\rvert \times 100$	16	7	22	16	16	16	16
$\left\lvert\frac{\tau_{Present}-\tau_{Smith\ and\ Teng\ (2001)}}{\tau_{Smith\ and\ Teng\ (2001)}}\right\rvert \times 100$	17	14	15	14	14	14	13

Parametric Study

An accurate understanding of RC composite beam behavior helps structural engineers optimize the design parameters. In this section, the most important effective design parameters in regard to the interfacial shear and normal stresses are explained.

Soffit Plate Stiffness

Fig. 8 shows the effect of stiffness on the interfacial shear and normal stresses in an RC beam strengthened by GFRP and CFRP sheets and a steel plate. The results show that as the soffit plate stiffness decreases and as we pass from the steel plate to the CFRP sheet and then to the GFRP sheet, the interfacial stresses decrease as well. Therefore, the soffit plate stiffness is an important parameter in determining the interfacial shear and normal stresses distribution, especially at the end zone of the soffit plate.

Soffit Plate Thickness and Width

Fig. 9 shows the effect of the soffit plate thickness on the interfacial shear and normal stresses in an RC beam strengthened by a steel plate. Three different thicknesses of plates were used, i.e., 4, 8, and 16 mm. These results show that the soffit plate thickness is an important variable in determining the interfacial stress concentrations and their intensities. The interfacial shear and normal stresses increase proportionally as the thickness of the soffit plate increases.

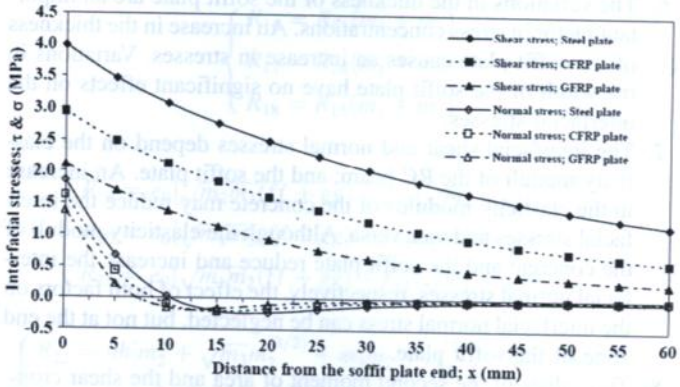

Fig. 8. Effect of the soffit plate stiffness on the interfacial shear and normal stresses in an RC beam strengthened by a GFRP/CFRP sheet or a steel plate

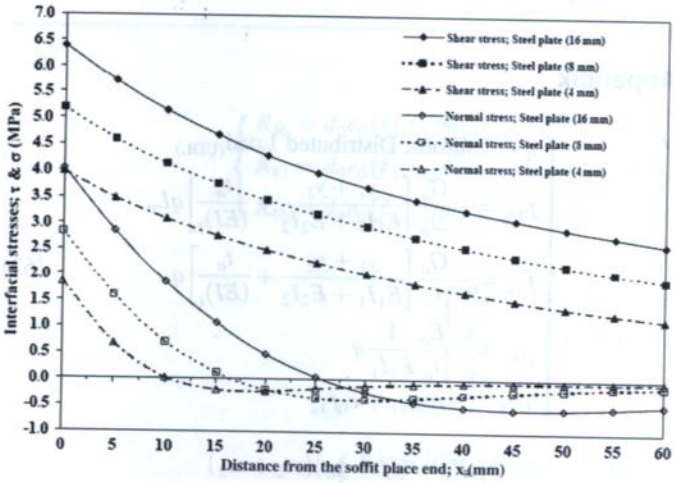

Fig. 9. Effect of the soffit plate thickness on the interfacial shear and normal stresses in an RC beam strengthened by a steel plate

Generally, in practical designs, the thicknesses of the GFRP and CFRP sheets are less than that of the steel plate. Therefore, the retrofitting and strengthening of structures by GFRP and CFRP sheets confer a comparative advantage in that they reduce the stress level and thus create a lower concentration of interfacial stress. Finally, the results show that the difference in the soffit plate width does not have a significant effect on the interfacial shear and normal stresses.

Adhesive Layer Thickness

Fig. 10 shows the effect of the thickness of the adhesive layer on the interfacial shear and normal stresses in a hollow aluminum beam strengthened by a CFRP sheet. Three different thicknesses—1, 2, and 4 mm—were used in this study. The results show that changing the adhesive layer thickness at the ends of the soffit plate has a considerable influence on the interfacial stresses.

Elasticity Moduli of the RC Beam and the Soffit Plate

Fig. 11 plots the distribution of the interfacial shear and normal stresses using three different values for the elasticity moduli—i.e., 20, 30, and 50 GPa—for an RC beam strengthened by a GFRP sheet. The diagrams show that an increase in the elasticity modulus leads to a reduction in the interfacial shear and normal stresses. This phenomenon happens because an important portion of the stress is absorbed by the principle beam when the elasticity modulus of the RC beam is increased. Therefore, a smaller portion of the stress is transferred to the adhesive layer and then to the soffit plate. Although the effect of the concrete elasticity modulus on

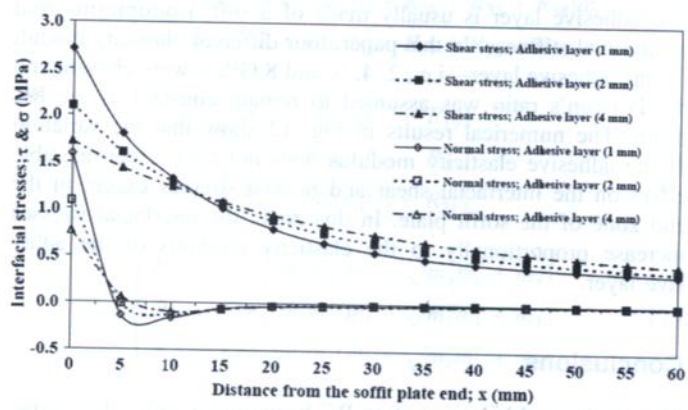

Fig. 10. Effect of the adhesive layer thickness on the interfacial shear and normal stresses in an Al beam strengthened by a CFRP sheet

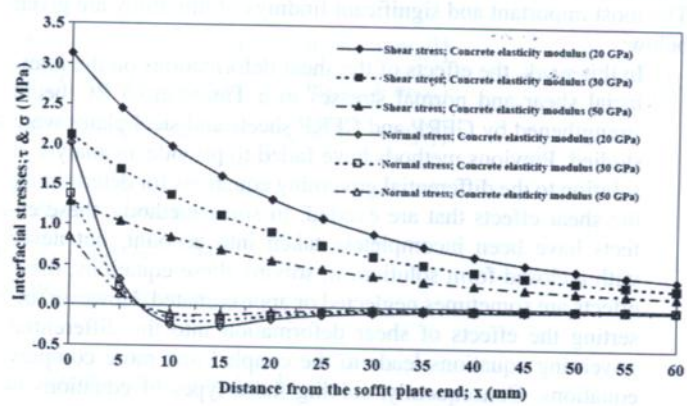

Fig. 11. Effect of the concrete elasticity modulus on the interfacial shear and normal stresses in an RC beam strengthened by a GFRP sheet

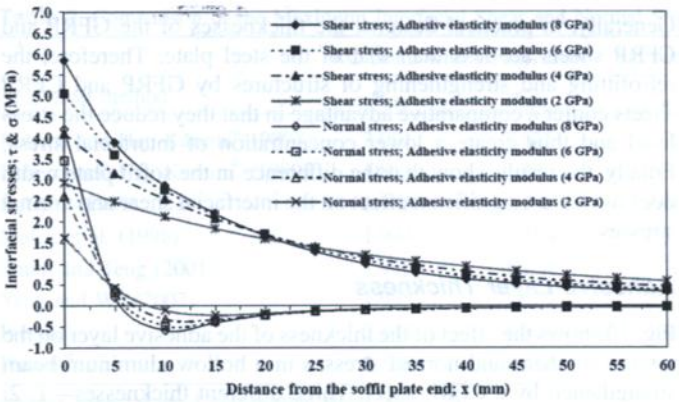

Fig. 12. Effect of the adhesive elasticity modulus on the interfacial shear and normal stresses in an RC beam strengthened by a CFRP sheet

the interfacial shear stress is considerable, one may neglect its effect on the normal stress, but not on the ends of the soffit plate. Investigations examining the variation of the elasticity modulus of the soffit plate show that, by increasing this parameter in a GFRP sheet, the values of the interfacial shear and normal stresses increase proportionally. The effect of this factor on the normal stress in the whole soffit plate may be fully neglected, with the exception of the end zone. Nevertheless, the investigation shows that the shear stresses are sensitive to the elasticity modulus of the soffit plate.

Elasticity Modulus of Adhesive Layer

The adhesive layer is usually made of a soft, isotropic material of minimal stiffness. In this paper, four different elasticity moduli for the adhesive layer—i.e., 2, 4, 6, and 8 GPa—were chosen, and the Poisson's ratio was assumed to remain constant in the RC beam. The numerical results in Fig. 12 show that the variation of the adhesive elasticity modulus does not have a considerable effect on the interfacial shear and normal stresses except in the end zone of the soffit plate. In this zone, the interfacial stresses increase proportionally to the elasticity modulus of the adhesive layer.

Conclusions

The mechanical behavior of an RC beam and a soffit plate, especially the distribution of the interfacial shear and normal stresses in the end zone of the connection between a concrete beam, an adhesive layer, and a soffit plate, depends on numerous factors. The most important and significant findings of this study are given below:

1. In this work, the effects of the shear deformations on the interfacial shear and normal stresses in a Timoshenko RC beam strengthened by GFRP and CFRP sheets and steel plates were studied. Previous methods have failed to provide an analytical solution to the differential governing equations for determining the shear effects that are exerted. In some methods, these effects have been incompletely taken into account, but never with a closed-form solution. In solving these equations, these effects are sometimes neglected or approximated. However, inserting the effects of shear deformation into the differential governing equations leads to the coupled and more complex equations. Consequently, solving these types of equations is more complicated. Despite this complication, an analytical solution was obtained for the interfacial shear and normal stresses in an RC beam strengthened by GFRP and CFRP sheets and steel plates. This solution is presented in this paper. This new presentation of the analytical solution has a general form and is applicable to any beam strengthened by GFRP or CFRP sheets or steel plates.
2. There is a considerable difference between the present analytical solution and previous solutions. In particular, the difference in the interfacial shear stresses is noticeable because these stresses are more sensitive to shear deformation.
3. Generally, the debonding phenomenon happens at the ends of the soffit plates. At these points, the interfacial shear and normal stresses between the concrete and adhesive layer reach their maximum values. Beyond this point, the shear stresses decrease as the distance from the end of plate increases, and it goes to zero at the midspan. Therefore, these stresses initiate the debonding phenomenon and the sudden failure of the structure. This is why the normal stresses are the main reason for the sudden variation in stiffness at the ends of the soffit plate.
4. A parametric study of the interfacial shear and normal stresses in the adhesive layer showed that these stresses at the ends of the soffit plate increase as the loads and the Young's modulus of the adhesive layer increase. However by increasing the thickness of the adhesive layer between the concrete and the soffit plate, the interfacial stress intensity can be reduced.
5. The interfacial shear and normal stresses decrease proportionally with respect to the reduction in stiffness.
6. The variations in the thickness of the soffit plate are an important factor in stress concentrations. An increase in the thickness of the soffit plate causes an increase in stresses. Variations in the width of the soffit plate have no significant effects on the interfacial stresses.
7. The interfacial shear and normal stresses depend on the elasticity moduli of the RC beam; and the soffit plate. An increase in the elasticity modulus of the concrete may reduce the interfacial stresses and vice versa. Although the elasticity moduli of the concrete and the soffit plate reduce and increase the interfacial normal stresses, respectively, the effect of both factors on the interfacial normal stress can be neglected, but not at the end zone of the soffit plate.
8. The values of the second moment of area and the shear cross-sectional area decrease because of both the shear deformation effect and the shear curvature in the composite beam. Therefore, the interfacial stresses may increase in both the soffit plate and the RC beam; that is, the tendency to slide between the soffit plate and the concrete interface is higher.

Appendix

$$\begin{cases} q = \text{Uniform Distributed Load}_{(\text{UDL})} \\ f_{11} = -\dfrac{G_a}{2t_a}\left[\dfrac{y_1+y_2}{E_1I_1+E_2I_2}+\dfrac{t_a}{(EI)_t}\right]qL_p \\ f_{12} = -\dfrac{G_a}{t_a}\left[\dfrac{y_1+y_2}{E_1I_1+E_2I_2}+\dfrac{t_a}{(EI)_t}\right]q \\ g_{11} = -\dfrac{E_a}{t_a}\dfrac{1}{E_1I_1}q \\ Cte = -a_0g_{11}+e_0f_{12} \end{cases} \tag{62}$$

$$\begin{cases} R_1 = (ff+gg)(m_2+m_3) \\ R_2 = (ff+gg)(m_1+m_3) \\ R_3 = (ff+gg)(m_1+m_2) \end{cases} \tag{63}$$

$$\begin{cases} R_4 = (ff+gg)m_2m_3 \\ R_5 = (ff+gg)m_1m_3 \\ R_6 = (ff+gg)m_1m_2 \end{cases} \tag{64}$$

$$\begin{cases} R_7 = (ff+gg)c_0^2 + [-R_1 + b_0(hh+mm)]c_0 \\ R_8 = (ff+gg)c_0^2 + [-R_2 + b_0(hh+mm)]c_0 \\ R_9 = (ff+gg)c_0^2 + [-R_3 + b_0(hh+mm)]c_0 \end{cases} \tag{65}$$

$$\begin{cases} R_{10} = hh(m_2 + \sqrt{m_3m_2} + m_3) + m_2mm \\ R_{11} = hh(m_1 + \sqrt{m_3m_1} + m_3) + m_1mm \\ R_{12} = hh(m_1 + \sqrt{m_2m_1} + m_2) + m_1mm \end{cases} \tag{66}$$

$$\begin{cases} R_{13} = (\sqrt{m_2} + \sqrt{m_3})(\sqrt{m_3}mm + nn + rr) \\ R_{14} = (\sqrt{m_1} + \sqrt{m_3})(\sqrt{m_3}mm + nn + rr) \\ R_{15} = (\sqrt{m_1} + \sqrt{m_2})(\sqrt{m_2}mm + nn + rr) \end{cases} \tag{67}$$

$$\begin{cases} W_1 = d_0[R_4 + R_7 - b_0(R_{10} + R_{13})]a_0^3 \\ W_2 = d_0[R_5 + R_8 - b_0(R_{11} + R_{14})]a_0^3 \\ W_3 = d_0[R_6 + R_9 - b_0(R_{12} + R_{15})]a_0^3 \end{cases} \tag{68}$$

$$\begin{cases} R_{16} = R_{13}(m_2 + m_3) \\ R_{17} = R_{14}(m_1 + m_3) \\ R_{18} = R_{15}(m_1 + m_2) \end{cases} \tag{69}$$

$$\begin{cases} R_{19} = e_0[\sqrt{m_2m_3}(ff+gg) + f_{11}(\sqrt{m_2} + \sqrt{m_3})] \\ R_{20} = e_0[\sqrt{m_1m_3}(ff+gg) + f_{11}(\sqrt{m_1} + \sqrt{m_3})] \\ R_{21} = e_0[\sqrt{m_1m_2}(ff+gg) + f_{11}(\sqrt{m_1} + \sqrt{m_2})] \end{cases} \tag{70}$$

$$\begin{cases} R_{22} = hh[m_2^2 + \sqrt{m_3}m_2^{(3/2)} + m_3m_2 + m_3^{(3/2)}\sqrt{m_2} + m_3^2] \\ R_{23} = hh[m_1^2 + \sqrt{m_3}m_1^{(3/2)} + m_3m_1 + m_3^{(3/2)}\sqrt{m_1} + m_3^2] \\ R_{24} = hh[m_1^2 + \sqrt{m_2}m_1^{(3/2)} + m_2m_1 + m_2^{(3/2)}\sqrt{m_1} + m_2^2] \end{cases} \tag{71}$$

$$\begin{cases} R_{25} = d_0(c_0^2 + m_2m_3)(f_{12} + R_1) \\ R_{26} = d_0(c_0^2 + m_1m_3)(f_{12} + R_2) \\ R_{27} = d_0(c_0^2 + m_1m_2)(f_{12} + R_3) \end{cases} \tag{72}$$

$$\begin{cases} R_{28} = d_0(m_2 + m_3)(f_{12} + R_1) \\ R_{29} = d_0(m_1 + m_3)(f_{12} + R_2) \\ R_{30} = d_0(m_1 + m_2)(f_{12} + R_3) \end{cases} \tag{73}$$

$$\begin{cases} R_{31} = e_0(ff+gg) + R_{10} \\ R_{32} = e_0(ff+gg) + R_{11} \\ R_{33} = e_0(ff+gg) + R_{12} \end{cases} \tag{74}$$

$$\begin{cases} R_{34} = [-Ctem_2m_3 - d_0(mmm_2{}^2 + R_{16} - R_{19} + R_{22})]b_0 \\ R_{35} = [-Ctem_1m_3 - d_0(mmm_1^2 + R_{17} - R_{20} + R_{23})]b_0 \\ R_{36} = [-Ctem_1m_2 - d_0(mmm_1^2 + R_{18} - R_{21} + R_{24})]b_0 \end{cases} \tag{75}$$

$$\begin{cases} R_{37} = c_0[b_0(d_0(R_{13} + R_{31}) - Cte\sqrt{m_2m_3}) - R_{28}] \\ R_{38} = c_0[b_0(d_0(R_{14} + R_{32}) - Cte\sqrt{m_1m_3}) - R_{29}] \\ R_{39} = c_0[b_0(d_0(R_{15} + R_{33}) - Cte\sqrt{m_1m_2}) - R_{30}] \end{cases} \tag{76}$$

$$\begin{cases} W_4 = [d_0e_0(hh+mm)b_0^2 + R_{25} + R_{34} + R_{37}]a_0^2 \\ W_5 = [d_0e_0(hh+mm)b_0^2 + R_{26} + R_{35} + R_{38}]a_0^2 \\ W_6 = [d_0e_0(hh+mm)b_0^2 + R_{27} + R_{36} + R_{39}]a_0^2 \end{cases} \tag{77}$$

$$\begin{cases} R_{40} = d_0(e_0f_{12} - R_{19}) \\ R_{41} = d_0(e_0f_{12} - R_{20}) \\ R_{42} = d_0(e_0f_{12} - R_{21}) \end{cases} \tag{78}$$

$$\begin{cases} R_{43} = Cte\sqrt{m_2m_3}(m_2 - \sqrt{m_3m_2} + m_3) \\ R_{44} = Cte\sqrt{m_1m_3}(m_1 - \sqrt{m_3m_1} + m_3) \\ R_{45} = Cte\sqrt{m_1m_2}(m_1 - \sqrt{m_2m_1} + m_2) \end{cases} \tag{79}$$

$$\begin{cases} R_{46} = d_0e_0\{f_{11}(\sqrt{m_2} + \sqrt{m_3})(m_2 + m_3) + \sqrt{m_2m_3}[f_{12} + (ff+gg)(m_2 + \sqrt{m_3m_2} + m_3)]\} \\ R_{47} = d_0e_0\{f_{11}(\sqrt{m_1} + \sqrt{m_3})(m_1 + m_3) + \sqrt{m_1m_3}[f_{12} + (ff+gg)(m_1 + \sqrt{m_3m_1} + m_3)]\} \\ R_{48} = d_0e_0\{f_{11}(\sqrt{m_1} + \sqrt{m_2})(m_1 + m_2) + \sqrt{m_1m_2}[f_{12} + (ff+gg)(m_1 + \sqrt{m_2m_1} + m_2)]\} \end{cases} \tag{80}$$

$$\begin{cases} R_{49} = d_0(c_0 - m_2)(c_0 - m_3)[R_4 + f_{12}(m_2 + m_3)] \\ R_{50} = d_0(c_0 - m_1)(c_0 - m_3)[R_5 + f_{12}(m_1 + m_3)] \\ R_{51} = d_0(c_0 - m_1)(c_0 - m_2)[R_6 + f_{12}(m_1 + m_2)] \end{cases} \tag{81}$$

$$\begin{cases} R_{52} = [Cte\sqrt{m_2m_3}c_0^2 + (R_{40} - R_{43})c_0 - Ctem_2m_3(m_2 + m_3) + R_{46}]b_0 \\ R_{53} = [Cte\sqrt{m_1m_3}c_0^2 + (R_{41} - R_{44})c_0 - Ctem_1m_3(m_1 + m_3) + R_{47}]b_0 \\ R_{54} = [Cte\sqrt{m_1m_2}c_0^2 + (R_{42} - R_{45})c_0 - Ctem_1m_2(m_1 + m_2) + R_{48}]b_0 \end{cases} \tag{82}$$

$$\begin{cases} W_7 = (-Ctee_0\sqrt{m_2m_3}b_0^2 + R_{52} + R_{49})a_0 \\ W_8 = (-Ctee_0\sqrt{m_1m_3}b_0^2 + R_{53} + R_{50})a_0 \\ W_9 = (-Ctee_0\sqrt{m_1m_2}b_0^2 + R_{54} + R_{51})a_0 \end{cases} \tag{83}$$

$$\begin{cases} W_{10} = (b_0Cte - d_0f_{12})\sqrt{m_2m_3}[(c_0 - m_2)\sqrt{m_2m_3}(c_0 - m_3) + b_0e_0(-c_0 + m_2 + m_3 + \sqrt{m_2m_3})] \\ W_{11} = (b_0Cte - d_0f_{12})\sqrt{m_1m_3}[(c_0 - m_1)\sqrt{m_1m_3}(c_0 - m_3) + b_0e_0(-c_0 + m_1 + m_3 + \sqrt{m_1m_3})] \\ W_{12} = (b_0Cte - d_0f_{12})\sqrt{m_1m_2}[(c_0 - m_1)\sqrt{m_1m_2}(c_0 - m_2) + b_0e_0(-c_0 + m_1 + m_2 + \sqrt{m_1m_2})] \end{cases} \tag{84}$$

$$\begin{cases} Z_1 = (a_0 - m_1)(W_1 - W_4 + W_7 + W_{10}) \\ Z_3 = -(a_0 - m_2)(W_2 - W_5 + W_8 + W_{11}) \\ Z_5 = (a_0 - m_3)(W_3 - W_6 + W_9 + W_{12}) \end{cases} \tag{85}$$

$$\begin{cases} S_1 = a_0^2b_0d_0(\sqrt{m_1} - \sqrt{m_2})(\sqrt{m_1} - \sqrt{m_3}) \\ S_2 = a_0^2b_0d_0(\sqrt{m_1} - \sqrt{m_2})(\sqrt{m_2} - \sqrt{m_3}) \\ S_3 = a_0^2b_0d_0(\sqrt{m_1} - \sqrt{m_3})(\sqrt{m_2} - \sqrt{m_3}) \end{cases} \tag{86}$$

$$\begin{cases} S_4 = c_0 + \sqrt{m_1}(\sqrt{m_2} + \sqrt{m_3}) + \sqrt{m_2m_3} \\ S_5 = (S_4(c_0 - m_1 - m_2 - m_3) - b_0e_0)a_0 \\ S_6 = (\sqrt{m_1} + \sqrt{m_2})(-c_0 + m_1 + m_2)m_3^{(3/2)} + \sqrt{m_1m_2}(-c_0 + m_1 + m_2 + \sqrt{m_1m_2})m_3 \\ S_7 = b_0e_0(-c_0 + m_1 + m_2 + \sqrt{m_1m_2} + \sqrt{m_3}) + m_3 + \sqrt{m_2m_3}) \\ S_8 = (c_0 - m_1)(c_0 - m_2)(\sqrt{m_1}(\sqrt{m_2} + \sqrt{m_3}) + \sqrt{m_2m_3}) \end{cases} \tag{87}$$

$$\begin{cases} M_1 = S_1(S_4a_0^2 + S_5 + S_6 + S_7 + S_8) \\ M_3 = S_2(S_4a_0^2 + S_5 + S_6 + S_7 + S_8) \\ M_5 = S_3(S_4a_0^2 + S_5 + S_6 + S_7 + S_8) \end{cases} \tag{88}$$

$$\begin{cases} C_1 = \dfrac{Z_1}{M_1} \\ C_3 = \dfrac{Z_3}{M_3} \\ C_5 = \dfrac{Z_5}{M_5} \end{cases} \tag{89}$$

Acknowledgments

The work described in this paper was fully supported by a research grant via Ferdowsi University of Mashhad (FUM). The authors are grateful for the financial support. Also the first author is thankful to Ilam University for his study assignment.

References

Antes, H. (2003). "Fundamental solution and integral equations for timoshenko beams." *Comput. Struct.*, 81(6), 383–396.

Chajes, M. J., Thomson, T. A., Jr., Januszka, T. F., and Finch, W. W., Jr. (1994). "Flexural strengthening of concrete beams using externally bonded composite materials." *Constr. Build. Mater.*, 8(3), 191–201.

Chen, J. F., and Teng, J. G. (2001). "Anchorage strength models for FRP and steel plates bonded to concrete." *J. Struct. Eng., ASCE*, 127(7), 784–791.

Cowper, G. R. (1966). "The shear coefficient in Timoshenko's beam theory." *J. Appl. Mech., ASCE*, 33(2), 335–340.

Etman, E. E., and Beeby, A. W. (2000). "Experimental programme and analytical study of bond stress distributions on a composite plate bonded to a reinforced concrete beam." *Cem. Conc. Compos.*, 22(4), 281–291.

Gere, J. M., and Timoshenko, S. P. (1984). "Mechanics of materials." *Brooks/Cole Engineering Division*, Monterey, CA.

Li, L. J., Guo, Y. C., Huang, P. Y., Liu, F., Deng, J., and Zhu, J. (2009). "Interfacial stress analysis of RC beams strengthened with hybrid CFS and GFS." *Constr. Build. Mater.*, 23(6), 2394–2401.

Maalej, M., and Bian, Y. (2001). "Interfacial shear stress concentration in FRP-strengthened beams." *Compos. Struct.*, 54(4), 417–426.

Maalej, M., and Leong, K. S. (2005). "Effect of beam size and FRP thickness on interfacial shear stress concentration and failure mode of FRP-strengthened beams." *Compos. Sci. Technol.*, 65(7–8), 1148–1158.

Malek, A. M., Saadatmanesh, H., and Ehsani, M. R. (1998). "Prediction of failure load of R/C beams strengthened with FRP plate due to stress concentration at the plate end." *ACI Struct. J.*, 95(2), 142–152.

Oehlers, D. J. (1992). "Reinforced concrete beams with plates glued to their soffits." *J. Struct. Eng., ASCE*, 118(8), 2023–2038.

Oehlers, D. J., and Moran, J. P. (1990). "Premature failure if externally plated reinforced concrete beams." *J. Struct. Eng., ASCE*, 116(4), 978–995.

Rabinovitch, O., and Frostig, Y. (2000). "Closed-form high-order analysis of RC beams strengthened with FRP strips." *J. Compos. Constr., ASCE*, 4(2), 65–74.

Rabinovitch, O., and Frostig, Y. (2001). "Delamination failure of RC beams strengthened with FRP strip—a closed-form high-order and fracture mechanics approach." *J. Eng. Mech.*, 127(8), 852–861.

Roberts, T. M. (1989). "Approximate analysis of shear and normal stress concentrations in the adhesive layer of plated RC beams." *Struct. Eng. Part A*, 67(12), 229–233.

Roberts, T. M., and Haji-Kazemi, H. (1989). "Theoretical study of the behavior of reinforced concrete beams strengthened by externally bonded steel plates." *Proc., Institution of Civil Engineers, Paper 9344, Structural Engineering Group, Part 2*, 87, 39–55.

Saadatmanesh, H., and Ehsani, M. R. (1991). "RC beams strengthened with GFRP plates. I: Experimental study." *J. Struct. Eng., ASCE*, 117(11), 3417–3433.

Saadatmanesh, H., and Malek, A. M. (1998). "Design guidelines for flexural strengthening of RC beams with FRP plates." *J. Compos. Constr., ASCE*, 2(4), 158–164.

Shen, H. S., Teng, J. G., and Yang, J. (2001). "Interfacial stresses in beams and slabs bonded with thin plate." *J. Eng. Mech., ASCE*, 127(4), 399–406.

Smith, S. T., and Teng, J. G. (2001). "Interfacial stresses in plated beams." *Eng. Struct.*, 23(7), 857–871.

Stafford, S. B., and Coull, A. (1991). *Tall building structures: Analysis and Design*, Wiley, New York.

Taljsten, B. (1997). "Strengthening of beams by plate bonding." *J. Mater. Civ. Eng., ASCE*, 9(4), 206–212.

Teng, J. G., Zhang, J. W., and Smith, S. T. (2002). "Interfacial stresses in reinforced concrete beams bonded with a soffit plate: a finite element study." *Constr. Build. Mater.*, 16(1), 1–14.

Tounsi, A. (2006). "Improved theoretical solution for interfacial stresses in concrete beams strengthened with FRP plate." *Int. J. Solids Struct.*, 43(14–15), 4154–4174.

Tounsi, A., Hassaine, D. T., Benyoucef, S., and Adda, B. E. A. (2009). "Interfacial stresses in FRP-plated RC beams: Effect of adherend shear deformations." *Int. J. Adhesion Adhesives*, 29(4), 343–351.

Vilnay, O. (1988). "The analysis of reinforced concrete beams strengthened by epoxy bonded steel plates." *Int. J. Cem. Compos. Lightweight Conc.*, 10(2), 73–78.

Wu, Z. S., Yuan, H., Kojima, Y., and Ahmed, E. (2005). "Experimental and analytical studies on peeling and spalling resistance of unidirectional FRP sheets bonded to concrete." *Compos. Sci. Technol.*, 65(7–8), 1088–1097.

Yang, J., Chen, J. F., and Teng, J. G. (2009). "Interfacial stresses analysis of plated beams under symmetric mechanical and thermal loading." *Constr. Build. Mater.*, 23(9), 2973–2987.

Yang, J., and Wu, Y. F. (2007). "Interfacial stresses of FRP strengthened concrete beams: Effect of shear deformation." *Compos. Struct.*, 80(3), 343–351.

Yang, Q. S., Peng, X. R., and Kwan, A. K. H. (2004). "Finite element analysis of interfacial stresses in FRP-RC hybrid beams." *Mech. Res. Commun.*, 31(3), 331–340.

Ye, J. Q. (2001). "Interfacial shear transfer of RC beams strengthened by bonded composite plates." *Cem. Conc. Compos.*, 23(4–5), 411–417.

Yuan, H., Chen, J. F., Teng, J. G., and Lu, X. Z. (2007). "Interfacial stress analysis of a thin plate bonded to a rigid substrate and subjected to inclined loading." *Int. J. Solids Struct.*, 44(16), 5247–5271.

Zhang, L., and Teng, J. G. (2010). "Finite element prediction of interfacial stresses in structural members bonded with a thin plate." *Eng. Struct.*, 32(2), 459–471.